

Transition-Metal Complexes Containing Parent Phosphine or Phosphinyl Ligands and Their Use as Precursors for Phosphide Nanoparticles

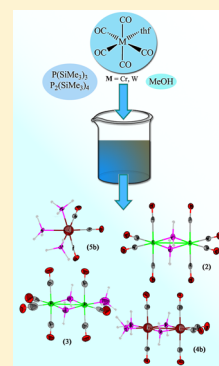
Susanne Bauer,[†] Cornelia Hunger,[†] Michael Bodensteiner,[†] Wilfried-Solo Ojo,[‡] Arnaud Cros-Gagneux,[‡] Bruno Chaudret,[‡] Céline Nayral,[‡] Fabien Delpech,[‡] and Manfred Scheer^{*†}

[†]Institut für Anorganische Chemie, Universität Regensburg, Universitätsstrasse 31, Regensburg, D-93053 Germany

[‡]INSA, UPS, CNRS; LPCNO (Laboratoire de Physique et Chimie des Nano-Objets), Université de Toulouse, 135 Avenue de Rangueil, F-31077 Toulouse, France

Supporting Information

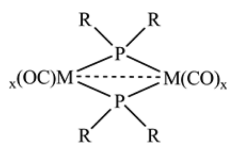
ABSTRACT: P–H functional transition-metal complexes were synthesized without using hazardous PH₃ gas in good yields by photolysis of the transition-metal carbonyl complexes M(CO)_{6-x} (M = Cr, W, Fe; x = 0, 1) in tetrahydrofuran followed by reaction with P₂(SiMe₃)₄ and subsequent methanolysis to give the bridging complexes [(CO)_xM(μ-PH₂)₂]₂ (M = Fe, x = 3 (1), M = Cr, x = 4 (2a), M = W, x = 4 (2b)). The photolysis of [(CO)₄M(μ-PH₂)₂]₂ (M = Cr (2a), M = W (2b)) with P(SiMe₃)₃ was applied followed by methanolysis to synthesize the PH₂ bridging transition-metal binuclear complexes with terminal PH₃ groups. The products [(CO)₄M(μ-PH₂)₂M(CO)₃(PH₃)]₂ (M = Cr (3a), M = W (3b)) and [(CO)₄W(μ-PH₂)₂W(CO)₂(PH₃)₂]₂ (4b) were isolated in moderate yield. Another synthetic approach to this type of compounds is the direct photolysis of the complexes [(CO)₃M(PH₃)₃]₂ (M = Cr (5a), M = W (5b)). The products were comprehensively characterized by ³¹P NMR and IR spectroscopy as well as by X-ray structural analysis. Additionally, the relevancy of 2a as single source precursor for the synthesis of stoichiometry-controlled CrP nanoparticles has been demonstrated.



INTRODUCTION

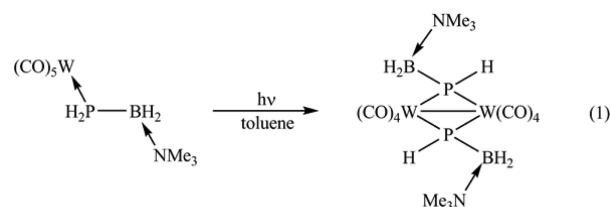
Phosphine complexes of transition-metal carbonyls are a prominent class of compounds; however, only a few contain the parent PH₃ ligand. Several binuclear complexes of the composition [(CO)_xM(μ-PR₂)₂]₂ have been reported (Scheme 1), among them only very few contain bridging PH₂ ligands

Scheme 1. Selected Examples of Compounds of the Type [(CO)_xM(μ-PR₂)₂]₂ (x = 4; M = V; R = Me; M = Cr; R = Me, Ph; M = Mo; R = Et; M = Mn; R = Me; M = W; R = Et,⁴ Ph,^{6,8} Me;⁸ x = 3; M = Fe; R = Me,¹¹ Ph^{9,10})



[(CO)₄Mn(μ-PH₂)₂]₂ (x = 2, 3).¹ Recently, we have shown that the photolysis of [(CO)₄Fe(PH₃)₃]₂ results in a complex with such a structural motif (e.g., [(CO)₃Fe(μ-PH₂)₂]₂) in high yields.² Furthermore, we have reported the synthesis of the binuclear complex [(CO)₄W(μ-PHR)]₂ containing bridging PHR ligands (R = H₂BNMe₃), which was obtained by the photolysis of the Lewis acid/base stabilized phosphanylborane complex [(CO)₅W·PH₂BH₂·NMe₃] (eq 1).³

In addition to these neutral complexes, some anionic derivatives have been reported, for example, [(CO)₄M]₂(μ-



PR₂)₂]²⁻ (M = Cr, Mo, W; R = Me, Ph)⁵⁻⁸ and [(CO)₃Fe]₂(μ-PPH₂)₂]^{2-,9,10}

Besides these homonuclear compounds, mixed bimetallic complexes of the type [(CO)₄M(μ-EMe₂)₂Fe(CO)₃]₂ (M = Cr, Mo, W; E = P, As)¹¹ and [(CO)₄M(μ-PMe₂)₂M'(CO)₄]₂ (M = Mo; M' = W)¹² are also known. Using the latter compound as a single source precursor in a MOCVD (metal-organic chemical vapor deposition) process, Basato et al. have deposited films with the stoichiometry predetermined by the precursor (Mo:W = 1:1).¹² However, they have not succeeded in avoiding the contamination of carbon in the films. Generally, the use of such single source precursors in the synthesis of transition-metal phosphide nanoparticles or films can yield highly selective compositions, but the appearance of carbon is also often a problem in these syntheses.

To avoid and minimize the concentration of carbon in these films, we developed the use of complexes which contain only

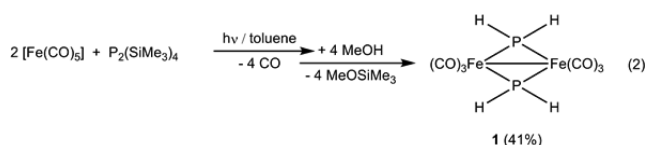
Received: May 27, 2014

Published: October 20, 2014

the needed elements and carbonyl groups as ligands.^{13,14} This can be furthermore achieved using complexes of the type $[(\text{CO})_x\text{M}(\mu\text{-PH}_2)]_2$ ($\text{M} = \text{Fe}$, $x = 3$) with bridging PH_2 ligands.² Note that it has been shown by the Whitmire group that the use of PH units in carbonyl clusters gives better results for nanoparticles than organosubstituted RP groups.^{15,16} Herein, we report the synthesis and characterization of the binuclear complexes $[(\text{CO})_4\text{M}(\mu\text{-PH}_2)]_2$, $[(\text{CO})_4\text{M}(\mu\text{-PH}_2)_2\text{M}(\text{CO})_3(\text{PH}_3)]$, and $[(\text{CO})_4\text{M}(\mu\text{-PH}_2)_2\text{M}(\text{CO})_2(\text{PH}_3)_2]$ ($\text{M} = \text{Cr}$, W), and their potential use for the generation of phosphide nanoparticles. We and others groups have shown that the single source approach using organometallic phosphide precursors provides a pertinent route to prepare phase-pure nanomaterials¹⁷ as exemplified in recent years for iron phosphides.^{2,15,16} We here demonstrate that this strategy can be extended to other transition-metal phosphides such as CrP for which to the best of our knowledge, no example of nanoparticles has been previously described in the literature.

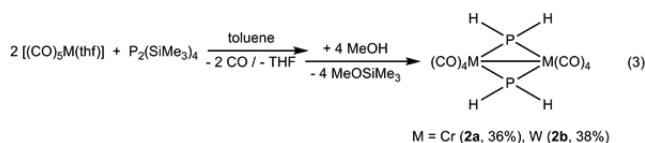
RESULTS AND DISCUSSION

We have previously reported the synthesis of $[(\text{CO})_3\text{Fe}(\mu\text{-PH}_2)]_2$ (**1**) by the photolysis of $[(\text{CO})_4\text{Fe}(\text{PH}_3)]_2$.² An alternative synthetic route for a CF_3 containing complex $[(\text{CO})_4\text{W}(\mu\text{-P}(\text{CF}_3)_2)]_2$ has been described by Dobbie et al.¹⁸ who obtained this product in very low yields (3%) by thermolysis of $\text{W}(\text{CO})_6$ with the corresponding diphosphane $\text{P}_2(\text{CF}_3)_4$. By using a related method, we successfully synthesized the binuclear iron complex $[(\text{CO})_3\text{Fe}(\mu\text{-PH}_2)]_2$ (**1**) by photolysis of $[\text{Fe}(\text{CO})_5]$ and $\text{P}_2(\text{SiMe}_3)_4$ in toluene followed by methanolysis (eq 2).¹⁹ In $\text{P}_2(\text{SiMe}_3)_4$ the PH_2



moieties are preformed. The ³¹P NMR spectrum of the crude reaction mixture shows $[(\text{CO})_4\text{Fe}(\text{PH}_3)]$ and $[(\text{CO})_3\text{Fe}(\mu\text{-PH}_2)]_2$ in a 30:70 ratio. To purify and isolate **1**, a column chromatographic workup was necessary, which decreases the isolated yield to 41%, but it is comparable to the yield of the previously described synthetic method.²

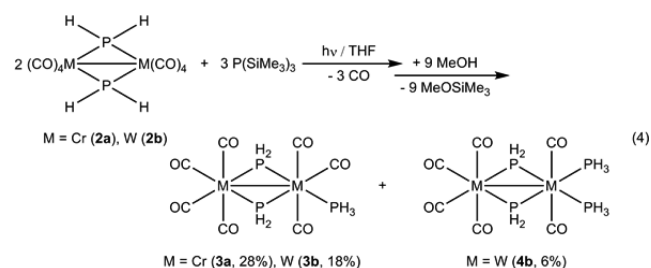
The analogue reaction of $[(\text{CO})_5\text{M}(\text{thf})]$ ($\text{M} = \text{Cr}$, W) with $\text{P}_2(\text{SiMe}_3)_4$ and subsequent methanolysis results in the formation of the complexes $[(\text{CO})_4\text{M}(\mu\text{-PH}_2)]_2$ ($\text{M} = \text{Cr}$



(**2a**), W (**2b**)) (eq 3) in similar yields as obtained for **1**. The ³¹P NMR spectrum of the crude reaction mixture shows $[(\text{CO})_5\text{M}(\text{PH}_3)]/[(\text{CO})_4\text{M}(\mu\text{-PH}_2)]_2$ in a 20/80 ratio for both metal complexes. After chromatographic workup, **2a** and **2b** are isolated in yields of 36% and 38%, respectively.

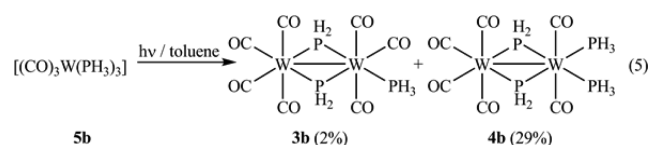
The binuclear complexes **1** and **2** possess exclusively carbonyl ligands as terminal ligands. Thus, the question arises, if it is also possible to introduce PH_3 ligands in terminal positions. Organo-substituted complexes at the P atoms have been already described.^{20,21} For example, $[(\text{CO})_4\text{W}(\mu\text{-}$

$\text{PEt}_2)_2\text{W}(\text{CO})_3(\text{PBu}_3)]$ and $[(\text{PBu}_3)(\text{CO})_3\text{W}(\mu\text{-PEt}_2)_2\text{W}(\text{CO})_3(\text{PBu}_3)]$ can be obtained by the thermolysis of $[(\text{CO})_4\text{W}(\mu\text{-PEt}_2)]_2$ with 2 and 4 equiv of PBu_3 , respectively.²⁰ Thus, the photolysis of **2** with 4 equiv of $\text{P}(\text{SiMe}_3)_3$ and subsequent methanolysis yields the complexes $[(\text{CO})_4\text{M}(\mu\text{-PH}_2)_2\text{M}(\text{CO})_3(\text{PH}_3)]$ ($\text{M} = \text{Cr}$ (**3a**), W (**3b**)) and $[(\text{CO})_4\text{M}(\mu\text{-PH}_2)_2\text{M}(\text{CO})_2(\text{PH}_3)_2]$ ($\text{M} = \text{W}$ (**4b**)) (eq 4); **3** is the main



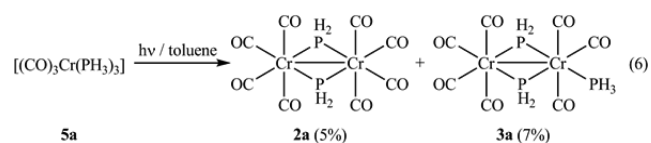
product while **4** represents the byproduct. Consequently the ³¹P NMR spectrum of the crude reaction mixture shows a product ratio **2a**:**3a** = 2:7 and **2b**:**3b**:**4b** of 17:65:18, respectively. Additionally, there are no indications for the existence of a third product such as $[(\text{PH}_3)(\text{CO})_3\text{M}(\mu\text{-PH}_2)_2\text{M}(\text{CO})_3(\text{PH}_3)]$, which would be the analogue of the reported complex $[(\text{PBu}_3)(\text{CO})_3\text{W}(\mu\text{-PEt}_2)_2\text{W}(\text{CO})_3(\text{PBu}_3)]$.²⁰ After chromatographic workup, **3** and **4** are obtained in yields of 28% (**3a**), 18% (**3b**), and 6% (**4b**), respectively.

Another route to synthesize **3b** and **4b** is the photolysis of $[(\text{CO})_3\text{W}(\text{PH}_3)_3]$ (**5b**) in toluene (eq 5). The starting material



was synthesized similarly to the previously reported preparation of $[(\text{CO})_4\text{W}(\text{PH}_3)_2]$.²² For reaction 5, **3b** is the byproduct and **4b** the main product. The ³¹P NMR spectrum of the crude reaction mixture shows **5b**:**3b**:**4b** in a 8:20:72 ratio. After column chromatographic workup, **3b** and **4b** are obtained in yields of 2% (**3b**) and 29% (**4b**), respectively.

In contrast to the photolysis of **5b**, the photolysis of $[(\text{CO})_3\text{Cr}(\text{PH}_3)_3]$ (**5a**) yields solely complexes **2a** and **3a** (eq 6) but not **4a** ($[(\text{CO})_4\text{Cr}(\mu\text{-PH}_2)_2\text{Cr}(\text{CO})_2(\text{PH}_3)_2]$). The ³¹P



NMR spectrum of the reaction mixture shows **5a**:**2a**:**3a** in a 46:11:43 ratio, and after column chromatographic workup, the products are obtained in low yields (**2a**, 5%; **3a**, 7%). Therefore, the photolysis of **5a** is not an appropriate alternative route for the synthesis of **2a** and **3a**.

Characterization and Spectroscopic Properties. The analytical data of **1** have been already reported.² Compounds **2a**, **2b**, **3a**, **3b**, **4b**, and **5b** are soluble in polar solvents and moderately soluble in nonpolar solvents. The color of **2a** and **3a** is green; **2b**, **3b**, and **4b** are red; and **5b** is colorless. In the EI mass spectra of **2a** and **2b**, the appropriate molecular ion

peaks are found, followed by a characteristic fragmentation pattern due to successive elimination of CO and H. In the $^{31}\text{P}\{^1\text{H}\}$ NMR spectrum of **2a** a singlet is observed which gives a triplet in the ^1H coupled spectrum. In comparison to **2a** the $^{31}\text{P}\{^1\text{H}\}$ NMR spectrum of **2b** shows a singlet with tungsten satellites, and in the ^{31}P NMR spectrum a multiplet of higher order spin system is detected.

In the EI mass spectrum of **3a** and **3b**, the molecular ion peak can be detected as well as characteristic fragmentation pattern by successive loss of CO, PH_3 , and H_2 . The difference between the EI mass spectra is that in **3a** first the PH_3 elimination occurs followed by the successive CO and H_2 elimination. For **3b** the CO elimination takes place first followed by PH_3 elimination. Accordingly, this might be the explanation for why it is not possible to synthesize the chromium derivate **4a** in which two carbonyl groups are substituted by two terminal PH_3 groups, but it was possible to synthesize and characterize the corresponding tungsten derivative **4b**. The $^{31}\text{P}\{^1\text{H}\}$ NMR spectrum of **3a** shows two doublets and one doublet of doublets which belongs to the terminal phosphorus moiety while the $^{31}\text{P}\{^1\text{H}\}$ NMR spectrum of **3b** shows three doublet of doublets. The ^{31}P NMR spectrum of **3a** reveals a triplet of doublets (P1'), a triplet of doublets of quartets (P1), and a quartet of doublets of doublets of triplets for the terminal phosphorus atom (P2) (Figures 1 and 3). In the ^1H NMR spectrum of **3a** and **3b** two doublets of doublets and one doublet can be detected.

The EI mass spectrum of **4b** shows the molecular ion peak as well as the characteristic fragmentation patters of successive elimination of PH_3 and CO. The $^{31}\text{P}\{^1\text{H}\}$ NMR spectrum of **4b** exhibits two multiples of a higher order spin system which are further split in the ^{31}P NMR spectrum. The ^1H NMR spectrum reveals also two multiples of a higher order spin system.

The data for **5a** are identical with the values described in the literature.²³ In the $^{31}\text{P}\{^1\text{H}\}$ NMR spectrum a singlet with tungsten satellites is observed which gives a multiplet of higher order in the ^1H coupled spectrum. The ^1H NMR spectrum shows also a multiplet of a higher order spin system. All NMR spectra have been simulated.

Crystal Structure Analysis. Single crystals of **2a** and **2b** were obtained from concentrated dichloromethane solutions at -25°C and crystallize in the orthorhombic space group $Cmca$. The central structural motif of **2a** and **2b** is a planar M_2P_2 four-membered ring with a M–M bond (M = Cr, W). In **2a** the distance of the Cr1–Cr1' bond is 2.929(3) Å and is comparable with the Cr–Cr distance reported for $[(\text{CO})_4\text{Cr}(\text{PMe}_2)_2]$ (2.905 Å).⁹ The W1–W1' bond length in **2b** is 3.068(3) Å and only slightly longer than the W–W distance in $[(\text{CO})_8\text{W}_2(\mu\text{-PHBH}_2\text{-NMe}_3)_2]$ (3.040(1) Å).³ The bond angles in M_2P_2 is $78.5(1)^\circ$ (Cr1–P1–Cr1') and $101.4(9)^\circ$ (P1–Cr1–P1') for **2a** (Figure 2) and $76.9(1)^\circ$ (W1–P1–W1') and $103.1(1)^\circ$ (P1–W1–P1') for **2b**. The coordination sphere of each metal atom is completed with four terminal carbonyl ligands. Each metal atom fulfills the 18 valence electron rule. The Cr–P bond length to the bridging phosphanido ligands is 2.314(9) Å and thus similar to those found in $[(\text{CO})_4\text{Cr}(\text{PMe}_2)_2]$ (2.318(2) Å).⁹ The W–P distance in **2b** is with 2.467(2) Å slightly shorter than the W–P distance in the published complex $[(\text{CO})_8\text{W}_2(\mu\text{-PHBH}_2\text{-NMe}_3)_2]$ (2.501(3) Å).³

Compound **3a** was crystallized from a dichloromethane solution at -25°C as dark green needles. Red needles of **3b** were obtained from a concentrated dichloromethane solution at

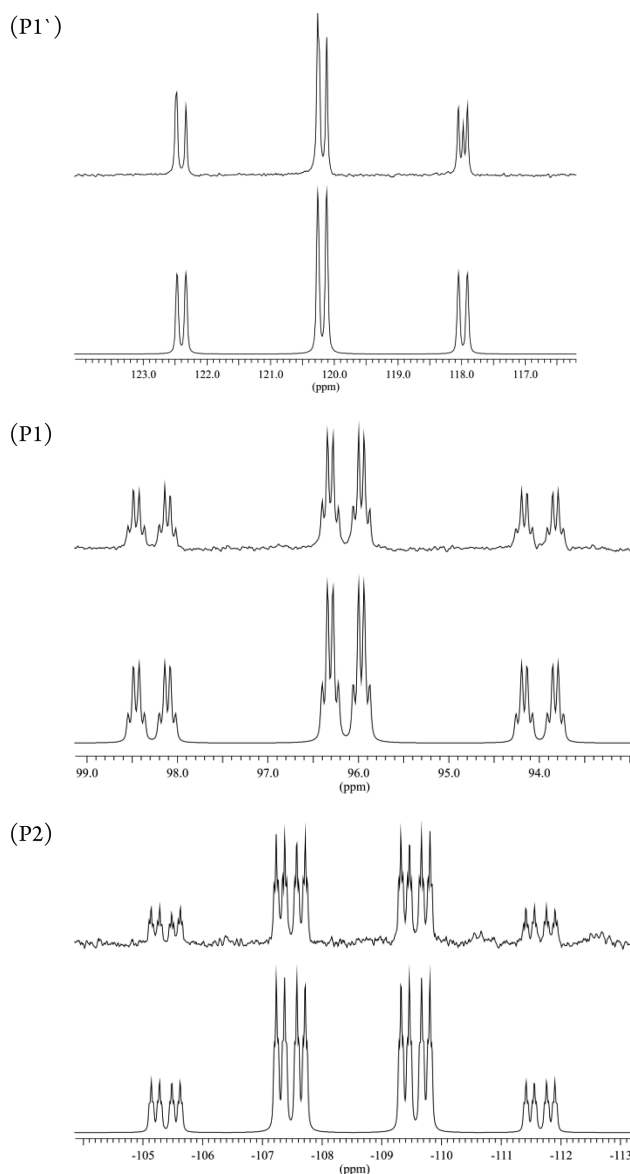


Figure 1. Experimental (C_6D_6 , 300 K, top) and simulated (bottom) ^{31}P NMR spectra of **3a** (the labeling of **3a** is shown in Figure 3).

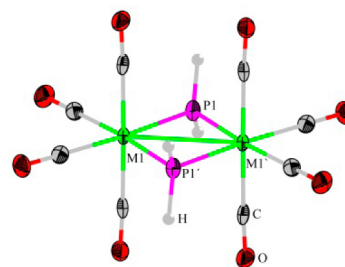


Figure 2. Molecular structure of **2a** (M = Cr) with thermal ellipsoids at a 50% probability level and **2b** (M = W), respectively. Selected bond lengths (Å) and angles (deg): Cr1–Cr1' 2.929(3), Cr1–P1 2.314(9), Cr1–P1' 2.314(9), Cr1–P1–Cr1' $78.5(1)$, P1–Cr1–P1' $101.4(9)$ (**2a**); W1–W1' 3.068(3), W1–P1 2.467(2), W1–P1' 2.467(2), W1–P1–W1' $76.9(1)$, P1–W1–P1' $103.1(1)$ (**2b**).

-25°C . The obtained single crystals crystallize in the triclinic space group $P\bar{1}$. The central structural motif of **3a** and **3b** is a planar M_2P_2 four-membered ring with an M–M bond (M = Cr,

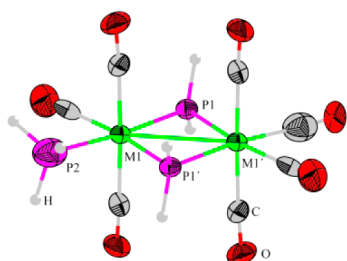


Figure 3. Molecular structure of **3a** ($M = \text{Cr}$) with thermal ellipsoids at a 50% probability level and **3b** ($M = \text{W}$). Selected bond lengths (Å) and angles [deg]: Cr1–Cr1' 2.9487(11), Cr1–P1 2.3111(10), Cr1–P1' 2.3087(9), Cr1–P2 2.265(6), Cr1–P3 2.23(2) Cr1–P1–Cr' 179.33(3), P1–Cr1–P1' 100.67(3) (**3a**); W1–W1' 3.0632(12), W1–P1 2.455(4), W1–P1' 2.459(3), W1–P2 2.454(4), W1–P3 2.41(4), W1–P1–W' 177.13(10), P1–W1–P1' 107.87(11) (**3b**).

W). On one of the metal atoms a terminal PH_3 group is bound beside three terminal CO groups. In **3a** the Cr1–Cr1' bond is 2.9487(11) Å and therefore in the range of **2a** (2.9293(5) Å). The Cr–P bond lengths to the bridging phosphanido atoms (Cr1–P1 2.3111(10) and Cr1–P1' 2.3087(9)) are comparable with the ones in **2a**. Only the Cr–P bond to the terminal phosphorus atom is with 2.265(6) and 2.23(2) Å (Cr1–P2 32%, Cr1–P3 18%) slightly shorter. In **3b** the W1–W1' distance (3.0632(12) Å) does not significantly differ from the ones in **2b** (3.068(3) Å). Also, here the W–P bond lengths to the bridging phosphanido atoms (W1–P1 2.455(4) and W1–P1' 2.459(3) Å) are only slightly longer than the bond length to the terminal phosphorus atom (W1–P2 2.454(4) Å, 36% and W1–P3 2.41(4) Å, 14%) but comparable with the corresponding distances in **3a**. The bond angles in the M_2P_2 four-membered ring are 79.33(3)° (Cr1–P1–Cr1') and 100.67(3)° (P1–Cr1–P1') for **3a** and 77.13(10)° (W1–P1–W1') and 102.87(11)° (P1–W1–P1') for **3b**.

Red prisms of **4b** grown from a dichloromethane solution at -25°C were suitable for X-ray crystallography and crystallize in the triclinic space group $P\bar{1}$. The central structural feature of **4b** (Figure 4) is a planar M_2P_2 four-membered ring. The

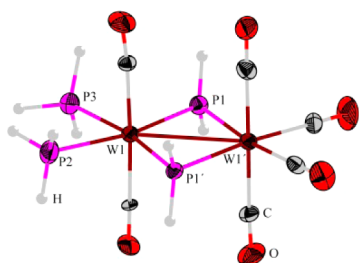


Figure 4. Molecular structure of **4b** with thermal ellipsoids at a 50% probability level. Selected bond lengths (Å) and angles (deg): W1–W1' 3.078(5), W1–P1 2.392(4), W1–P1' 2.402, W1–P2 2.463(4), W1–P3 2.452(4), P1–W1–P1' 104.13(13), P1–W1'–P1' 99.36(13), W1–P1–W1' 78.22(12), W1–P1'–W1' 78.29(12).

coordination sphere of one tungsten atom is completed by four terminal carbonyl ligands. On the other tungsten atom two terminal carbonyls and two terminal PH_3 ligands are bound which are trans located to the bridging PH_2 groups. The W1–W1' distance of 3.078(5) Å is similar to the W–W bond length in **3b** (3.0632(12) Å). The distances between the tungsten and the terminal phosphorus atoms are 2.463(4) and 2.452(4) Å and, hence, are similar to the $\text{W–P}_{\text{terminal}}$ bond length in **3b**

(2.454(4) Å). The distances to the bridging phosphanido atoms are at 2.392(4) and 2.403(4) Å smaller than the distance in **3b** (2.455(4) and 2.459(3) Å) and can be explained by the lower trans influence of the bridging PH_2 ligands in comparison to the CO ligands. Due to the different coordination sphere of the tungsten atoms, there are different P–W–P angles. The P1–W1–P1' angle (104.13(13)°) is enlarged in comparison to the smaller P1–W1'–P1' angle with 99.36(13)°. The W1–P1'–W1' angles are found to be 78.22(12)° and 78.29(12)° resulting in an overall value of 360° in the W_2P_2 four-membered ring.

E. O. Fischer and U. Klabunde synthesized the transition-metal complexes **5a** and **5b** by using PH_3 gas.^{23,24} Now it was possible for the first time to prepare **5a** and **5b** on a new synthetic route without using the toxic PH_3 gas. Because the structure of **5a** was described in the literature,^{25,26} a X-ray structure analysis was only performed for **5b**. The compound crystallizes in the monoclinic space group $P2_1/m$. The molecular structure of **5b** (Figure 5) can be described as

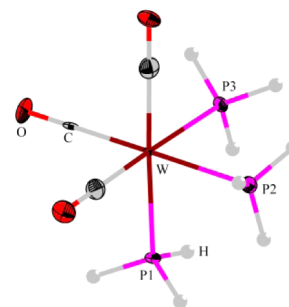


Figure 5. Molecular structure of **5b** with thermal ellipsoids at a 50% probability level. Selected bond lengths (Å) and angles (deg): W–P1 2.486(7), W–P2 2.486(7), W–P3 2.492(2), P1–W–P2 87.8(1), P2–W–P3 89.4(7), P1–W–P3 89.4(7).

octahedral with three carbonyl and three PH_3 ligands in a facial arrangement coordinating to the central tungsten atom. The W–P bond lengths are 2.456(7) and 2.454(3) Å and comparable with the corresponding bond lengths in $[(\text{CO})_4\text{W}(\text{PH}_3)_2]$ (2.492(1) and 2.493(5) Å) and $[(\text{CO})_5\text{W}(\text{PH}_3)]$ (2.491(2) Å).^{20,27} The bond angle P1–W–P2 87.8(1)° and P1–W–P3 89.4(7)° are also in the expected range (cf., $[(\text{CO})_4\text{W}(\text{PH}_3)_2]$ with 86.8(6)°).²⁰

Synthesis of Chromium Phosphide Nanoparticles. The bulk phase diagram of chromium and phosphorus shows at least six known chromium phosphides compounds (Cr_3P , Cr_2P , Cr_2P_7 , CrP , CrP_2 , CrP_4).²⁸ At the nanoscale, only thin films of CrP and Cr_3P have been previously prepared, with CrP being the most promising phase in terms of potential applications (hard-wearing metallic conductor resistant to oxidation, electrode for battery).²⁹ In our case, the CrP nanoparticles (NPs) were prepared via the thermolysis of the single source dinuclear complex **2a**. In a typical reaction, **2a** and hexadecylamine (HDA) together with oleic acid (OIA) as ligands are dissolved in mesitylene and maintained at 180°C for 1 h. As evidenced by transmission electron microscopy (TEM) (Figure 6) and high resolution (HRTEM) (Supporting Information), individual particles of mean diameter 4.3(0.7) nm are prepared. Featureless X-ray diffraction pattern (Supporting Information) shows that these NPs are amorphous. The synthesis can be achieved at lower temperature (150°C), but irregularly shaped nanoparticles are then obtained (Supporting Information).

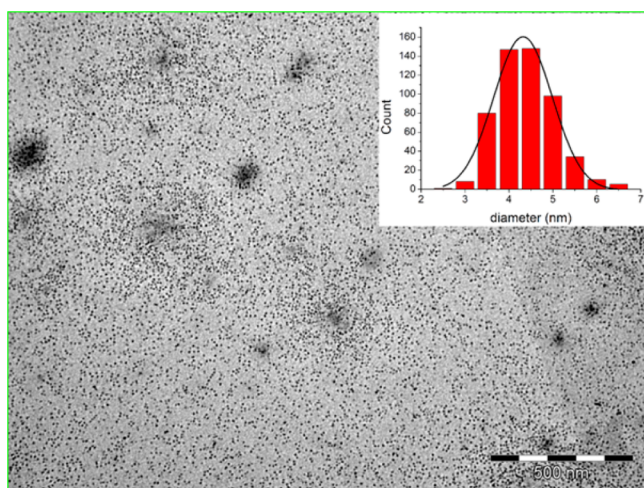


Figure 6. TEM and size distribution (inset) of CrP nanoparticles prepared from **2a** in the presence of 1 equiv of HDA and OLA.

Remarkably, and in contrast to many reported attempts in the chemistry of metal phosphide NPs,^{15,16,30} the composition of the obtained NPs (analyzed by ICP-MS and TEM-EDS, see Supporting Information) matches the 1:1 metal–phosphorus content of the precursor with precise stoichiometry control. Beside Cr and P, they also contain ca. 80% of organic species as determined by elemental analysis. ¹H NMR spectroscopy was employed to probe the surface environment and ligand composition. The ¹H NMR spectrum is shown in Supporting Information and allows quantifying the respective amount of HDA and oleate (using the alkene protons and the methyl protons around 5.4 and 0.9 ppm) that is close to the introduced ratio 1:1 (1:0.94). The possible presence of the phosphine ligand at the surface was discarded on the basis of the ³¹P{¹H} MAS NMR spectrum which shows that the only phosphorus species are the Cr–P phosphides (Supporting Information). The strong coordination of these ligands results in resonance broadening (of the ethylene protons at ~5.4 ppm and of the methylene ones located α to the C=C double bond at ~2.0 ppm) which becomes more pronounced for protons closer to the surface.³¹ As a consequence, the methylene protons located

Table 1. Crystallographic Details

	1	2a	2b	3a	3b	4b	5b
CCDC	1002518	1002519	1002520	1002521	1002522	1002523	1002524
formula	C ₆ H ₄ Fe ₂ O ₆ P ₂	C ₈ H ₄ Cr ₂ O ₈ P ₂	C ₈ H ₄ O ₈ P ₂ W ₂	C ₇ H ₇ Cr ₂ O ₇ P ₃	C ₇ H ₇ O ₇ P ₃ W ₂	C ₆ H ₁₀ O ₆ P ₄ W ₂	C ₃ H ₉ O ₃ P ₃ W
$D_{\text{calc}}/\text{g cm}^{-3}$	1.961	1.895	2.868	1.833	2.876	2.832	2.476
μ/mm^{-1}	2.755	15.499	15.328	15.728	30.530	30.682	25.853
fw	345.73	394.05	657.73	400.04	663.74	669.70	369.85
color	yellow	black	red	green	red	orangish red	colorless
shape	prism	block	prism	plate	rod	stick	parallelepiped
max size/mm	0.42	0.19	0.25	0.56	0.12	0.12	0.28
mid size/mm	0.27	0.19	0.20	0.15	0.07	0.04	0.15
min size/mm	0.22	0.11	0.12	0.01	0.03	0.02	0.08
T/K	123(1)	123(1)	123(1)	123(1)	123(1)	123(1)	123(1)
cryst syst	monoclinic	orthorhombic	orthorhombic	triclinic	triclinic	triclinic	monoclinic
space group	$P2_1/m$	C_{mca}	C_{mca}	$P\bar{1}$	$P\bar{1}$	$P\bar{1}$	$P2_1/m$
$a/\text{\AA}$	6.2476(7)	12.2545(3)	12.4977(12)	6.9134(9)	7.0082(10)	7.0140(14)	6.3812(1)
$b/\text{\AA}$	12.9819(11)	11.5949(3)	12.0462(14)	7.3239(10)	7.4298(10)	9.3860(19)	11.3455(2)
$c/\text{\AA}$	7.2193(8)	9.7196(2)	10.1185(9)	8.7610(10)	8.8711(13)	13.632(3)	6.8708(1)
α/deg	90	90	90	111.796(12)	111.050(13)	70.15(3)	90
β/deg	90.135(14)	90	90	92.150(10)	92.726(12)	79.82(3)	94.207(2)
γ/deg	90	90	90	115.204(14)	114.076(13)	68.78(3)	90
$V/\text{\AA}^3$	585.53(10)	1381.06(6)	1523.3(3)	362.42(9)	383.24(11)	785.4(4)	496.091(14)
Z	2	4	4	1	1	2	2
Z'	0.5	0.25	0.25	0.5	0.5	1	0.5
$\Theta_{\text{min}}/\text{deg}$	3.26	6.96	3.09	5.592	5.487	3.45	6.46
$\Theta_{\text{max}}/\text{deg}$	28.01	66.74	27.84	66.631	66.716	51.31	62.29
measured reflns	8337	4607	9212	4479	5585	4305	1659
indep reflns	1444	629	952	1250	1312	1679	790
reflns used	1414	590	789	1097	1224	1247	780
R_{int}	0.0273	0.0389	0.0479	0.0602	0.1595	0.0417	0.0416
params	84	54	52	112	117	169	57
restraints	0	0	0	12	61	36	6
largest peak	0.408	0.307	1.317	0.555	3.077	1.282	3.130
deepest hole	−0.314	−0.269	−0.640	−0.380	−3.033	−1.182	−2.639
GOF	1.284	1.097	1.104	1.053	1.081	1.002	1.094
wR2 (all data)	0.0753	0.0654	0.0558	0.1036	0.1638	0.0879	0.1392
wR2	0.0751	0.0645	0.0541	0.1004	0.1605	0.0859	0.1388
R1 (all data)	0.0263	0.0250	0.0275	0.0436	0.0637	0.0474	0.0526
R1	0.0258	0.0233	0.0229	0.0386	0.0609	0.0351	0.0523

α to the amine, as well as the methylene protons located α and β to the carboxylate functions, are not visible. The tight ligation is further supported by the diffusion-ordered NMR spectroscopy (DOSY) experiment and the self-coefficient diffusion of the ligands in CrP NPs which is significantly smaller ($1.6 \times 10^{-10} \text{ m}^2/\text{s}$) than those of the free forms of HDA ($9.4 \times 10^{-10} \text{ m}^2/\text{s}$) and OIA ($6.0 \times 10^{-10} \text{ m}^2/\text{s}$). Diffusion coefficients and hydrodynamic radii are correlated by the Stokes–Einstein relation $D = (kT)/(\delta\pi\eta r)$ (where D is the diffusion coefficient, k is the Boltzmann constant, T is the temperature in K, η is the viscosity of the solution, and r is the radius). The NP ligands' self-diffusion coefficient agrees with a hydrodynamic diameter of 4.6 nm, which is in agreement with the TEM value. The ratio between the amine, the acid, and the complex **2a** is of paramount importance for the morphology and the dispersion of NPs. For instance, the use of solely HDA or OIA results in agglomerated NPs (Supporting Information). When using both stabilizers but in lower quantities (0.5 or 0.1 equiv of each one), irregularly shaped NPs were obtained demonstrating insufficient steric constrain (Supporting Information). Thus, only the combination of 1 equiv of HDA and of OIA results in the formation of spherical nanoparticles indicating that the presence of both ligands in significant amount is required, presumably for inducing a soft but robust template.³²

CONCLUSIONS

The use of $\text{P}(\text{SiMe}_3)_3$ and $\text{P}_2(\text{SiMe}_3)_4$ in their reaction with transition-metal carbonyls and the subsequent methanolysis in a “one-pot-synthesis” opens a very convenient route for the synthesis of new parent phosphanide (PH_2^-) complexes of transition metals. The products can be used as single source precursors for the generation of transition-metal phosphides, as exemplified by the preparation of stoichiometry-controlled CrP nanoparticles. It is conceivable to synthesize new nano-objects using the suggested starting materials as single source precursors to create nanoparticles with novel properties which can be controlled by different stoichiometry and reaction conditions.

EXPERIMENTAL SECTION

General Techniques. The manipulations were carried out under dinitrogen using standard Schlenk techniques. All solvents were dried using standard procedures and were freshly distilled prior to use. The NMR spectra were recorded on a Bruker Avance 400 (^1H , 400.132 MHz; ^{31}P , 161.975 MHz) and Avance 500 (^1H , 500.332 MHz) with δ referenced to external SiMe_4 (^1H) or H_3PO_4 (^{31}P), respectively. The NMR spectra were simulated with the program WinDaisy.³³ Solid state NMR experiments were recorded on a Bruker Avance 400 spectrometer equipped with a 3.2 mm probe. Samples were spun at 16 kHz at the magic angle using ZrO_2 rotors. For ^1H magic angle spinning (MAS), and ^{31}P MAS single-pulse experiments, small flip angles ($\sim 30^\circ$) were used with recycle delays of 5 and 60 s. IR spectra were measured at a Varian FTS-800 spectrometer. Mass spectra were recorded on a Finnigan MAT SSQ 710 A (EI) spectrometer. Microscopy samples were prepared by deposition of a drop of diluted colloidal solution onto a carbon-coated copper grid and observed at the “Service Commun de Microscopie Electronique de l'Université Paul Sabatier” (TEMSCAN) on a JEOL 1011 microscope for bright-field transmission electronic microscopy (TEM), or a JEOL-2100F field-emission microscope for high resolution TEM (HRTEM), the latter two working at 100 and 200 kV, respectively. Elemental analyses (ICP-MS) were performed by Antellis Co. (Cr, P).

Synthesis of 1. A mixture of $[\text{Fe}(\text{CO})_5]$ (1.842 g, 9.41 mmol) and $\text{P}_2(\text{SiMe}_3)_4$ (1.668 g, 4.70 mmol) was irradiated in THF (60 mL) for 3 h. MeOH (1.848 g, 57.67 mmol) was added, and the mixture was

stirred for 14 h. Removing the solvent under reduced pressure yielded a red crude product, which was purified by column chromatography (SiO_2 , hexane). Elution with hexane yielded a yellow fraction, which was identified by NMR spectroscopy as the known complex $[(\text{CO})_4\text{Fe}(\text{PH}_3)]$. When the polarity was increased with toluene a yellow fraction of **1** could be eluted. Crystals were obtained by slow sublimation at room temperature at 10^{-3} mbar (see Table 1 for crystallographic details). Yield: 667 mg (41%). IR (KBr): ν_{CO} 2071(s), 2018(vs), 1995(vs) cm^{-1} ; ν_{PH} 2363(w), 2331(w) cm^{-1} . ^1H NMR (400.132 MHz, C_6D_6): $\delta = 0.48\text{--}3.49$ (m, $^1J_{\text{PH}} = 380.5$ Hz, $^1J_{\text{PH}} = 377.5$ Hz, $^3J_{\text{PH}} = 26.9$ Hz, $^3J_{\text{PH}} = 26.4$ Hz, $^2J_{\text{HH}} = 10.5$ Hz, $^4J_{\text{HH}} = 7.5$ Hz, $^4J_{\text{HH}} = 1.1$ Hz, $^4J_{\text{HH}} = 0.7$ Hz, 4 H, PH_2) (these coupling constants were obtained by NMR spectra simulation). $^{31}\text{P}\{^1\text{H}\}$ NMR (161.975 MHz, C_6D_6): $\delta = -10$ (s, PH_2). ^{31}P NMR (161.975 MHz, C_6D_6): $\delta = -10$ (m, $^2J_{\text{PP}} = 182.2$ Hz, $^1J_{\text{PH}} = 380.5$ Hz, $^1J_{\text{PH}} = 377.5$ Hz, $^3J_{\text{PH}} = 26.9$ Hz, $^3J_{\text{PH}} = 26.4$ Hz, PH_2) (these coupling constants were obtained by NMR spectra simulation). EI-MS (70 eV): m/z (%) = 346 (94) $[(\text{CO})_3\text{Fe}(\mu\text{-PH}_2)_2\text{Fe}(\text{CO})_3]^+$, 318 (71) $[(\text{CO})_3\text{Fe}(\mu\text{-PH}_2)_2\text{Fe}(\text{CO})_2]^+$, 290 (55) $[(\text{CO})_2\text{Fe}(\mu\text{-PH}_2)_2\text{Fe}(\text{CO})_2]^+$, 262 (55) $[(\text{CO})_2\text{Fe}(\mu\text{-PH}_2)_2\text{Fe}(\text{CO})]^+$, 234 (100) $[(\text{CO})\text{Fe}(\mu\text{-PH}_2)_2\text{Fe}(\text{CO})]^+$, 206 (99) $[(\text{CO})\text{Fe}(\mu\text{-PH}_2)_2\text{Fe}]^+$, 178 (95) $[\text{Fe}(\mu\text{-PH}_2)_2\text{Fe}]^+$. Anal. Calcd for $\text{C}_6\text{H}_4\text{Fe}_2\text{O}_6\text{P}_2$: C, 20.84; H, 1.17. Found: C, 20.45; H, 1.08.

Synthesis of 2a. A solution of $[(\text{CO})_5\text{Cr}(\text{thf})]$ in toluene was obtained, starting from $[(\text{CO})_5\text{Cr}(\text{thf})]^{34}$ (500 mL, 45.76 mmol/L, 22.88 mmol) in THF, which was replaced by stepwise evaporation of THF and subsequent addition of toluene (500 mL). To this solution $\text{P}_2(\text{SiMe}_3)_4$ (4.057 g, 11.44 mmol) dissolved in 25 mL toluene was added. After stirring for 1 week at room temperature, MeOH (1.466 g, 1.85 mL, 45.76 mmol) was added, and the mixture was stirred for an additional 14 h. Removing the solvent under reduced pressure yielded a brown crude product, which was initially extracted three times with 5 mL MeOH to remove the byproducts. Afterward the dark green residue was solved in 100 mL toluene and filtered. Removing the toluene, dissolving the residue in 20 mL CH_2Cl_2 , and storing at -25°C yielded **2a** as green crystals. Yield: 1.623 g (36%). IR (KBr): ν_{CO} 2013(s), 1996(m), 1953(vs), 1937(vs) cm^{-1} ; ν_{PH} 2369(w), 2357(w) cm^{-1} . ^1H NMR (400.132 MHz, C_6D_6): $\delta = 6.07$ (d, $^1J_{\text{PH}} = 363.8$ Hz, 4 H, PH_2). $^{31}\text{P}\{^1\text{H}\}$ NMR (161.975 MHz, C_6D_6): $\delta = 122$ (s, PH_2). ^{31}P NMR (161.975 MHz, C_6D_6): $\delta = 122$ (t, $^1J_{\text{PH}} = 363.8$ Hz, PH_2). EI-MS (70 eV): m/z (%) = 394 (48) $[(\text{CO})_4\text{Cr}(\mu\text{-PH}_2)(\mu\text{-PH}_2)\text{Cr}(\text{CO})_4]^+$, 366 (13) $[(\text{CO})_4\text{Cr}(\mu\text{-PH}_2)(\mu\text{-PH}_2)\text{Cr}(\text{CO})_3]^+$, 338 (59) $[(\text{CO})_3\text{Cr}(\mu\text{-PH}_2)(\mu\text{-PH}_2)\text{Cr}(\text{CO})_3]^+$, 310 (15) $[(\text{CO})_3\text{Cr}(\mu\text{-PH}_2)(\mu\text{-PH}_2)\text{Cr}(\text{CO})_2]^+$, 282 (65) $[(\text{CO})_2\text{Cr}(\mu\text{-PH}_2)(\mu\text{-PH}_2)\text{Cr}(\text{CO})_2]^+$, 254 (61) $[(\text{CO})_2\text{Cr}(\mu\text{-PH}_2)(\mu\text{-PH}_2)\text{Cr}(\text{CO})]^+$, 226 (100) $[(\text{CO})\text{Cr}(\mu\text{-PH}_2)(\mu\text{-PH}_2)\text{Cr}(\text{CO})]^+$, 198 (54) $[(\text{CO})\text{Cr}(\mu\text{-PH}_2)(\mu\text{-PH}_2)\text{Cr}]^+$, 170 (80) $[\text{Cr}(\mu\text{-PH}_2)(\mu\text{-PH}_2)\text{Cr}]^+$, 166 (35) $[\text{Cr}(\mu\text{-P})(\mu\text{-P})\text{Cr}]^+$. Anal. Calcd for $\text{C}_8\text{H}_4\text{O}_8\text{P}_2\text{Cr}_2$ (394.05 g/mol): C, 24.38; H, 1.02. Found C, 24.36; H, 1.03.

Synthesis of 2b. A solution of $[(\text{CO})_5\text{W}(\text{thf})]$ in toluene was obtained, starting from $[(\text{CO})_5\text{W}(\text{thf})]^{34}$ (500 mL, 34.2 mmol/L, 17.10 mmol) in THF, which was replaced by stepwise evaporation of THF and subsequent addition of toluene (500 mL). To this solution $\text{P}_2(\text{SiMe}_3)_4$ (3.033 g, 8.55 mmol) dissolved in 25 mL toluene was added. After the mixture stirred for 1 week at room temperature, MeOH (1.315 g, 1.66 mL, 41.04 mmol) was added, and the mixture was stirred for an additional 14 h. Removing the solvent under reduced pressure yielded a brown raw product, which was initially extracted three times with 5 mL of MeOH to remove the byproducts. Afterward the red residue was solved in 100 mL of toluene and filtered. Removing the toluene, dissolving the residue in 20 mL of CH_2Cl_2 , and storing at -25°C yielded **2b** as red crystals. Yield: 2.135 g (38%). IR (KBr): ν_{CO} 2025(s), 1993(m), 1957(vs), 1937(vs) cm^{-1} ; ν_{PH} 2383(w), 2369(w) cm^{-1} . ^1H NMR (400.132 MHz, C_6D_6): $\delta = 5.41$ (m, $^1J_{\text{PH}} = 391.7$ Hz, $^3J_{\text{PH}} = 0.5$ Hz, $^4J_{\text{HH}} = 3.0$ Hz, 4 H, PH_2) (these coupling constants were obtained by NMR spectra simulation). $^{31}\text{P}\{^1\text{H}\}$ NMR (161.975 MHz, C_6D_6): $\delta = 8$ (s, $^1J_{\text{PW}} = 164.8$ Hz, PH_2). ^{31}P NMR (161.975 MHz, C_6D_6): $\delta = 8$ (m, $^2J_{\text{PP}} = 1.5$ Hz, $^1J_{\text{PH}} = 391.7$ Hz, $^3J_{\text{PH}} = 0.5$ Hz, $^1J_{\text{PW}} = 164.8$ Hz, PH_2) (these coupling constants were obtained by NMR spectra simulation). EI-MS (70 eV): m/z (%)

= 658 (48) [(CO)₄W(μ-PH₂)(μ-PH₂W(CO)₄)⁺, 630 (42) [(CO)₄W(μ-PH₂)(μ-PH₂W(CO)₃)⁺, 600 (50) [(CO)₃W(μ-PH₂)(μ-P)W(CO)₃]⁺, 570 (100) [(CO)₃W(μ-P)(μ-P)W(CO)₂]⁺, 542 (40) [(CO)₂W(μ-P)(μ-P)W(CO)₂]⁺, 514 (43) [(CO)₂W(μ-P)(μ-P)W(CO)]⁺, 486 (49) [(CO)W(μ-P)(μ-P)W(CO)]⁺, 458 (49) [(CO)W(μ-P)(μ-P)W]⁺, 430 (95) [W(μ-P)(μ-P)W]⁺. Anal. Calcd for C₈H₄O₈P₂W₂ (657.74 g/mol): C, 14.61; H, 0.61. Found C, 14.97; H, 0.70.

Synthesis of 3a. A solution of [(CO)₄Cr(μ-PH₂)₂] (2a) (555 mg, 1.4 mmol) and P(SiMe₃)₃ (1.4 g, 5.6 mmol) in 50 mL of THF was irradiated for 9.5 h. MeOH in excess (0.7 mL) was added, and the mixture was stirred for 1 week at room temperature. Removing the solvent under reduced pressure yielded a brown crude product in which two compounds (2a and 3a) could be identified by ³¹P{¹H} NMR spectroscopy. They were separated by column chromatography (SiO₂, hexane). First a green fraction of 2a (135 mg, 34%) was eluted with hexane. The polarity was increased continuously with toluene. The next dark green fraction contains the main product 3a (160 mg, 28%) (hexane:toluene = 3:1.3). Green crystals of 3a were obtained by removing the solvent, dissolving the residue in 10 mL THF, and storing at –25 °C. Yield: 160 mg (28%). IR (KBr): ν_{CO} 2044(s), 2024(s), 2000(vs), 1938(vs), 1916(vs), 1880(sh) cm^{–1}; ν_{PH} 2354(w), 2350(w) cm^{–1}. ¹H NMR (400.132 MHz, C₆D₆): δ = 3.57 (dd, ¹J_{PH} = 339.2 Hz, ³J_{PH} = 9.9 Hz, 3 H, PH₃), 4.62 (dd, ¹J_{PH} = 347.7 Hz, ³J_{PH} = 5.9 Hz, 2 H, PH₂), 5.46 (d, ¹J_{PH} = 358.8 Hz, 2 H, PH₂) ppm (these coupling constants were obtained by NMR spectra simulation). ³¹P{¹H} NMR (161.975 MHz, C₆D₆): δ = –109 (dd, ²J_{PP} = 55.8 Hz, ²J_{PP} = 22.5 Hz, PH₃), 96 (d, ²J_{PP} = 55.8 Hz, PH₂), 120 (d, ²J_{PP} = 22.5 Hz, PH₂) ppm (these coupling constants were obtained by NMR spectra simulation). ³¹P NMR (161.975 MHz, C₆D₆): δ = –109 (qddt, ²J_{PP} = 55.8 Hz, ²J_{PP} = 22.5 Hz, ¹J_{PH} = 339.2 Hz, ³J_{PH} = 5.9 Hz, PH₃), 96 (tdq, ²J_{PP} = 55.8 Hz, ¹J_{PH} = 347.7 Hz, ³J_{PH} = 9.9 Hz, PH₂), 120 (td, ²J_{PP} = 22.5 Hz, ¹J_{PH} = 358.8 Hz, PH₂) ppm (these coupling constants were obtained by NMR spectra simulation). EI-MS (70 eV): *m/z* (%) = 400 (5) [(CO)₄Cr(μ-PH₂)₂Cr(CO)₃(PH₃)⁺, 366 (2) [(CO)₄Cr(μ-PH₂)₂Cr(CO)₃]⁺, 338 (28) [(CO)₃Cr(μ-PH₂)₂Cr(CO)₃]⁺, 310 (10) [(CO)₃Cr(μ-PH₂)₂Cr(CO)₂]⁺, 282 (55) [(CO)₂Cr(μ-PH₂)₂Cr(CO)₂]⁺, 254 (48) [(CO)₂Cr(μ-PH₂)₂Cr(CO)]⁺, 226 (84) [(CO)Cr(μ-PH₂)₂Cr(CO)]⁺, 198 (46) [(CO)Cr(μ-PH₂)₂Cr]⁺, 170 (100) [Cr(μ-PH₂)₂Cr]⁺, 166 (41) [Cr(μ-P)₂Cr]⁺. Anal. Calcd for C₇H₇O₇P₃Cr₂0.5C₄H₈O (435.09 g/mol): C, 24.8; H, 2.54. Found C, 25.13; H, 2.58.

Synthesis of 3b. A solution of [(CO)₄W(μ-PH₂)₂] (2b) (400 mg, 0.6 mmol) and P(SiMe₃)₃ (600 mg, 2.4 mmol) in 50 mL of THF was irradiated for 9.5 h. MeOH in excess (0.5 mL) was added, and the mixture was stirred for 14 h at room temperature. Removing the solvent under reduced pressure yielded a brown raw product in which three compounds (2b, 3b, and 4b) could be identified by ³¹P{¹H} NMR spectroscopy. They were separated by column chromatography (SiO₂, hexane). First a red fraction of 2b (135 mg, 34%) was eluted with hexane. The polarity was increased continuously with toluene. The next red fraction contains the main product 3b (70 mg, 18%) (n-hexane:toluene = 3:1). Finally small amounts of 4b (26 mg, 6%) in a third red fraction could be eluted with toluene. Red crystals of 3b were obtained by removing the solvent, dissolving the residue in 10 mL of CH₂Cl₂, and storing at –25 °C. Yield: 70 mg (18%). IR (KBr): ν_{CO} 2051(s), 2008(vs), 1940(br), 1907(vs), 1885(sh), 1870(vs) cm^{–1}; ν_{PH} 2362(w), 2345(w) cm^{–1}. ¹H NMR (400.132 MHz, C₆D₆): δ = 3.70 (dd, ¹J_{PH} = 354.9 Hz, ³J_{PH} = 10.3 Hz, 3 H, PH₃), 5.02 (dd, ¹J_{PH} = 373.6 Hz, ³J_{PH} = 4.3 Hz, 2 H, PH₂), 5.87 (d, ¹J_{PH} = 384.8 Hz, 2 H, PH₂) (these coupling constants were obtained by NMR spectra simulation). ³¹P{¹H} NMR (161.975 MHz, C₆D₆): δ = –186 (dd, ²J_{PP} = 38.7 Hz, ²J_{PP} = 34.3 Hz, ¹J_{PW} = 222.6 Hz, PH₃), –10 (dd, ²J_{PP} = 34.3 Hz, ²J_{PP} = 9.0 Hz, ¹J_{PW} = 178.6 Hz, ¹J_{PW} = 156.8 Hz, PH₂), 5 (dd, ²J_{PP} = 38.7 Hz, ²J_{PP} = 9.0 Hz, ¹J_{PW} = 211.1 Hz, ¹J_{PW} = 153.6 Hz, PH₂) (these coupling constants were obtained by NMR spectra simulation). ³¹P NMR (161.975 MHz, C₆D₆): δ = –186 (m, ²J_{PP} = 38.7 Hz, ²J_{PP} = 34.3 Hz, ¹J_{PH} = 354.9 Hz, ³J_{PH} = 4.3 Hz, ¹J_{PW} = 222.6 Hz, PH₃), –10 (m, ²J_{PP} = 34.3 Hz, ²J_{PP} = 9.0 Hz, ¹J_{PH} = 373.6 Hz, ³J_{PH} = 10.3 Hz, ¹J_{PW} = 178.6

Hz, ¹J_{PW} = 156.8 Hz, PH₂), 5 (dd, ²J_{PP} = 38.7 Hz, ²J_{PP} = 9.0 Hz, ¹J_{PH} = 384.8 Hz, ¹J_{PW} = 211.1 Hz, ¹J_{PW} = 153.6 Hz, PH₂) (these coupling constants were obtained by NMR spectra simulation). EI-MS (70 eV): *m/z* (%) = 664 (70) [(CO)₄W(μ-PH₂)₂W(CO)₃(PH₃)⁺, 636 (48) [(CO)₃W(μ-PH₂)₂W(CO)₃(PH₃)⁺, 602 (38) [(CO)₃W(μ-PH₂)₂W(CO)₃]⁺, 574 (100) [(CO)₃W(μ-PH₂)₂W(CO)₂]⁺, 546 (37) [(CO)₂W(μ-PH₂)₂W(CO)₂]⁺, 518 (40) [(CO)₂W(μ-PH₂)₂W(CO)]⁺, 490 (35) [(CO)W(μ-PH₂)₂W(CO)]⁺, 461 (95) [(CO)W(μ-PH₂)(μ-P)W]⁺, 430 (47) [W(μ-P)₂W]⁺. Anal. Calcd for C₇H₇O₇P₃W₂ (664.74 g/mol): C, 12.65; H, 1.21. Found C, 12.76; H, 1.08.

Photolysis of 5a. A solution of [(CO)₃Cr(PH₃)₃]²⁺ (5a) (1.40 g, 5.88 mmol) in 250 mL of toluene was irradiated for 12 h. Removing the solvent under reduced pressure yielded a brown raw product, in which three compounds could be identified by ³¹P{¹H} NMR spectroscopy, which were separated by column chromatography (SiO₂, hexane). The polarity was increased continuously with toluene. First there were small amounts of 2a (59 mg, 5.1%) in a green fraction. The next green zone contains small amounts of 3a (75 mg, 6.5%). The third orange zone contains the starting material 5a (153 mg, 11%).

Synthesis of 4b. A solution of [(CO)₃W(PH₃)₃]²⁺ (5b) (1.00 g, 2.70 mmol) in 200 mL of toluene was irradiated for 7 h. Removing the solvent under reduced pressure yielded a brown raw product, in which three compounds could be identified by ³¹P{¹H} NMR spectroscopy, which were separated by column chromatography (SiO₂, hexane). The polarity was increased continuously with toluene. First there were small amounts of 3b (13 mg, 1.5%), and then small amounts of 5b (72 mg, 7.1%) in the form of a red and a yellow zone, respectively. The next red zone contains the core product 4b (265 mg, 29.3%). Crystals were obtained by removing the solvent, dissolving 4b in 10 mL of CH₂Cl₂, and storing at –25 °C. Yield: 265 mg (29.3%). IR (KBr) ν_{CO} 2026(s), 1980(sh), 1965(vs), 1912(vs), 1895(vs), 1842(s) cm^{–1}; ν_{PH} 2360(s), 2343(m) cm^{–1}. ¹H NMR (400.132 MHz, C₆D₆): δ = 3.76 (m, ¹J_{PH} = 342.0 Hz, ³J_{PH} = 16.8 Hz, ³J_{PH} = 10.7 Hz, ³J_{PH} = 0.1 Hz, 6 H), 5.49 (m, ¹J_{PH} = 367.4 Hz, ³J_{PH} = 3.9 Hz, ³J_{PH} = 2.9 Hz, ³J_{PH} = 1.1 Hz, PH₂, 4 H) (these coupling constants were obtained by NMR spectra simulation). ³¹P{¹H} NMR (161.975 MHz, C₆D₆): δ = –166 (m, ²J_{PP} = 59.4 Hz, ²J_{PP} = 32.2 Hz, ²J_{PP} = 22.1 Hz, ¹J_{PW} = 211.6 Hz, ²J_{PW} = 5.3 Hz, PH₃), –11 (m, ²J_{PP} = 59.4 Hz, ²J_{PP} = 32.2 Hz, ²J_{PP} = 5.4 Hz, ¹J_{PW} = 223.4 Hz, ²J_{PW} = 98.9 Hz, PH₂) (these coupling constants were obtained by NMR spectra simulation). ³¹P NMR (161.975 MHz, C₆D₆): δ = –166 (m, ²J_{PP} = 59.4 Hz, ²J_{PP} = 32.2 Hz, ²J_{PP} = 22.1 Hz, ¹J_{PH} = 342.0 Hz, ³J_{PH} = 16.8 Hz, ³J_{PH} = 3.9 Hz, ³J_{PH} = 2.9 Hz, ¹J_{PW} = 211.6 Hz, ²J_{PW} = 5.3 Hz, PH₃), –11 (m, ²J_{PP} = 59.4 Hz, ²J_{PP} = 32.2 Hz, ²J_{PP} = 5.4 Hz, ¹J_{PH} = 342.0 Hz, ³J_{PH} = 16.8 Hz, ³J_{PH} = 3.9 Hz, ³J_{PH} = 2.9 Hz, ¹J_{PW} = 211.6 Hz, ²J_{PW} = 5.3 Hz, PH₃), –11 (m, ²J_{PP} = 59.4 Hz, ²J_{PP} = 32.2 Hz, ²J_{PP} = 5.4 Hz, ¹J_{PH} = 342.0 Hz, ³J_{PH} = 16.8 Hz, ³J_{PH} = 3.9 Hz, ³J_{PH} = 2.9 Hz, ¹J_{PW} = 211.6 Hz, ²J_{PW} = 5.3 Hz, PH₃), –11 (m, ²J_{PP} = 59.4 Hz, ²J_{PP} = 32.2 Hz, ²J_{PP} = 5.4 Hz, ¹J_{PW} = 223.4 Hz, ²J_{PW} = 98.9 Hz, PH₂) (these coupling constants were obtained by NMR spectra simulation). EI-MS (70 eV): *m/z* (%) = 670 (94) [(CO)₄W(μ-PH₂)₂W(CO)₂(PH₃)₂]⁺, 636 (44) [(CO)₄W(μ-PH₂)₂W(CO)₂(PH₃)]⁺, 608 (34) [(CO)₃W(μ-PH₂)₂W(CO)₂(PH₃)⁺, 580 (100) [(CO)₃W(μ-PH₂)₂W(CO)(PH₃)⁺, 552 (41) [(CO)₂W(μ-PH₂)₂W(CO)(PH₃)⁺, 518 (47) [(CO)₂W(μ-PH₂)₂W(CO)]⁺, 490 (72) [(CO)W(μ-PH₂)₂W(CO)]⁺, 462 (86) [(CO)W(μ-PH₂)₂W]⁺, 429 (26) [(CO)W(μ-PH₂)W]⁺, 401 (7) [W(μ-PH₂)W]⁺. Anal. Calcd for C₆H₁₀O₆P₄W₂ (670.72 g/mol): C, 10.76; H, 1.51. Found C, 11.01; H, 1.62.

Synthesis of 5a. A mixture of [(CO)₃Cr(NCPh)₃]³⁺ (5.00 g, 19.29 mmol) and P(SiMe₃)₃ (15.95 g, 63.666 mmol) was stirred in THF (150 mL) at room temperature for 30 min. MeOH (7.35 g, 0.229 mol) was added, and the mixture was stirred for 14 h. Removing the solvent yielded a brown crude product, which was extracted with 200 mL of toluene. After removal of the toluene, the orange powder was dried under vacuum. Crystals were obtained by dissolving the residue in 100 mL of toluene and storing at –25 °C. Yield: 2.63 g (57%). IR (toluene solution): ν_{CO} 1958(s), 1871(s) cm^{–1}; ν_{PH} 2307(w) cm^{–1}. ¹H NMR (400.132 MHz, C₆D₆): δ = 2.80 (m, ¹J_{PH} = 303.6 Hz, ³J_{PH} = 14.6 Hz, 9 H, PH₃) (these coupling constants were obtained by NMR spectra simulation). ³¹P{¹H} NMR (161.975 MHz, C₆D₆): δ = –109 (s, PH₃). ³¹P NMR (161.975 MHz, C₆D₆): δ = –109 (m, ²J_{PP} = 25.6 Hz, ¹J_{PH} = 303.6 Hz, ³J_{PH} = 14.6 Hz, PH₃) (these coupling constants were

obtained by NMR spectra simulation). EI-MS (70 eV): m/z (%) = 238 (89) $[(\text{CO})_3\text{Cr}(\text{PH}_3)_3]^+$, 210 (3) $[(\text{CO})_2\text{Cr}(\text{PH}_3)_3]^+$, 182 (5) $[(\text{CO})\text{Cr}(\text{PH}_3)_3]^+$, 154 (18) $[\text{Cr}(\text{PH}_3)_3]^+$, 120 (100) $[\text{Cr}(\text{PH}_3)_2]^+$, 86 (83) $[\text{Cr}(\text{PH}_3)]^+$, 52 (38) $[\text{Cr}]^+$. Anal. Calcd for $\text{C}_3\text{H}_9\text{O}_3\text{P}_3\text{Cr}$ (238.02 g/mol): C, 15.14; H, 3.81. Found C, 15.74; H, 3.81.

Synthesis of 5b. A mixture of $[(\text{CO})_3\text{W}(\text{NCPH}_3)]^{36}$ (6.128 g, 10.62 mmol) and $\text{P}(\text{SiMe}_3)_3$ (7.98 g, 31.85 mmol) was stirred in THF (150 mL) at room temperature for 30 min. MeOH (3.67 g, 0.115 mol) was added, and the mixture was stirred for 14 h. Reduction of the solvent to a volume of 40 mL and addition of Et_2O (80 mL) yielded a yellow precipitate. After the precipitate was filtered and washed with 10 mL of Et_2O and 10 mL of THF, it was dried under vacuum. Crystals were obtained by dissolving the residue in 100 mL of toluene and storing at -25°C . Yield: 2.63 g (21%). IR (toluene solution): ν_{CO} 1961(s), 1871(s) cm^{-1} ; ν_{PH} 2323(w) cm^{-1} . ^1H NMR (400.132 MHz, C_6D_6): δ = 3.01 (m, $^1J_{\text{PH}}$ = 316.5 Hz, $^3J_{\text{PH}}$ = 11.4 Hz, 9 H, PH_3) (these coupling constants were obtained by NMR spectra simulation). $^{31}\text{P}\{^1\text{H}\}$ NMR (161.975 MHz, C_6D_6): δ = -168 (s, $^1J_{\text{PW}}$ = 202.0 Hz, PH_3) ppm. ^{31}P NMR (161.975 MHz, C_6D_6): δ = -168 (m, $^2J_{\text{PP}}$ = 13.8 Hz, $^1J_{\text{PH}}$ = 316.5 Hz, $^3J_{\text{PH}}$ = 11.4 Hz, $^1J_{\text{PW}}$ = 202.0 Hz, PH_3) (these coupling constants were obtained by NMR spectra simulation). EI-MS (70 eV): m/z (%) = 370 (56) $[(\text{CO})_3\text{W}(\text{PH}_3)_3]^+$, 342 (18) $[(\text{CO})_2\text{W}(\text{PH}_3)_3]^+$, 314 (29) $[(\text{CO})\text{W}(\text{PH}_3)_3]^+$, 286 (10) $[\text{W}(\text{PH}_3)_3]^+$. Anal. Calcd for $\text{C}_3\text{H}_9\text{O}_3\text{P}_3\text{W}$ (369.86 g/mol): C, 9.74; H, 2.45. Found C, 9.97; H, 2.37.

CrP NPs synthesis. $[(\text{CO})_4\text{Cr}(\mu\text{-PH}_2)]_2$ (118.2 mg, 0.30 mmol), oleic acid (84.7 mg, 0.30 mmol), and hexadecylamine (71.4 mg, 0.30 mmol) were dissolved in 10 mL of mesitylene in a Fisher–Porter reactor. The mixture was heated at 180°C for 1 h. After the reacted solution cooled to room temperature, the black CrP NPs were obtained as a black precipitate after centrifugation. This powder was then washed with a mixture of toluene and methanol and dried under vacuum. Yield: 37 mg (15%).

■ ASSOCIATED CONTENT

■ Supporting Information

X-ray crystallographic data for the complexes **1**, **2**, **3**, **4b**, **5b**; EI mass spectra of **2**, **3**; experimental and simulated ^1H and ^{31}P NMR spectra of **2**, **3**, **4b**, **5b**; solution ^1H NMR spectrum of the CrP NPs; ^1H and ^{31}P MAS NMR spectra of the CrP NPs; TEM images of the CrP NPs using various combination of ligands; HRTEM image of the CrP NPs; HRTEM-EDS spectrum of CrP NPs; XRP-diffractogram of the CrP NPs; $^{31}\text{P}\{^1\text{H}\}$ NMR spectra of the decomposition of **2a**. This material is available free of charge via the Internet at <http://pubs.acs.org>. CCDC 1002518 (**1**), 1002519 (**2a**), 1002520 (**2b**), 1002521 (**3a**), 1002522 (**3b**), 1002523 (**4b**) and 1002524 (**5b**) contain the supplementary crystallographic data for this paper. These data can be obtained free of charge at www.ccdc.cam.ac.uk/conts/retrieving.html (or from the Cambridge Crystallographic Data Centre, 12 Union Road, Cambridge CB2 1EZ, U.K.; Fax: + 44-1223-336-033; e-mail: deposit@ccdc.cam.ac.uk).

■ AUTHOR INFORMATION

Corresponding Author

*E-mail: manfred.scheer@ur.de.

Author Contributions

The manuscript was written through contributions of all authors and finalized by the corresponding author. S.B. and C.H. contributed equally to the synthesis and characterization of the new products and performed the simulations of the NMR spectra. M.B. is responsible for the X-ray structural characterization. The French team did the generation and characterization of the NPs. All authors have given approval to the final version of the manuscript.

Notes

The authors declare no competing financial interest.

■ ACKNOWLEDGMENTS

This work was supported by the Deutsche Forschungsgemeinschaft and the University of Regensburg, the Université Paul Sabatier, the CNRS, and the Institut National des Sciences Appliquées de Toulouse. The authors thank the Région Midi-Pyrénées and the European Commission for the POCTEFA Interreg project (MET-NANO EFA 17/08). We thank Yannick Copp and Christian Bijani for NMR measurements and Angélique Gillet for her help.

■ REFERENCES

- (1) Deppisch, B.; Schaefer, H.; Binder, D.; Leske, W. Z. *Anorg. Allg. Chem.* **1984**, *519*, 53–66. For more literature of PH_3 and PH_2 containing complexes, see refs 19–24.
- (2) Dreher, C.; Ojo, W.-S.; Bauer, S.; Xu, S.; Zabel, Z.; Virieux, H.; Chaudret, B.; Lacroix, L.-M.; Scheer, M.; Nayral, C.; Delpech, F. *Chem. Commun.* **2013**, *49*, 11788–11790.
- (3) Vogel, U.; Hoemensch, P.; Schwan, K.-C.; Timoshkin, A. Y.; Scheer, M. *Chem.—Eur. J.* **2003**, *9*, 515–519.
- (4) Vahrenkamp, H. *Chem. Ber.* **1978**, *111*, 3472–3483.
- (5) Dessy, R. E.; Rheingold, A. L.; Howard, G. D. *J. Am. Chem. Soc.* **1972**, *94*, 746–752.
- (6) Keiter, R. L.; Madigan, M. J. *Organometallics* **1982**, *1*, 409–411.
- (7) Keiter, R. L.; Madigan, M. J. *J. Organomet. Chem.* **1987**, *331*, 341–346.
- (8) Keiter, R. L.; Keiter, E. A.; Rust, M. S.; Miller, D. R.; Sherman, E. O.; Cooper, D. E. *Organometallics* **1992**, *11*, 487–489.
- (9) Ginsburg, R. E.; Rothrock, R. K.; Finke, R. G.; Collman, J. P.; Dahl, L. F. *J. Am. Chem. Soc.* **1979**, *101*, 6550–6562.
- (10) Collman, J. P.; Rothrock, R. K.; Finke, R. G.; Moore, E. J.; Rose-Munch, F. *Inorg. Chem.* **1982**, *21*, 146–156.
- (11) Trenkle, A.; Vahrenkamp, H. *J. Organomet. Chem.* **1982**, *236*, 71–81.
- (12) Basato, M.; Brescacin, E.; Tondello, E.; Valle, G. *Inorg. Chim. Acta* **2001**, *323*, 147–151.
- (13) Vogel, U.; Scheer, M. *Phosphorus, Sulfur Silicon Relat. Elem.* **2001**, *168–169*, 547–550.
- (14) Scheer, M.; Vogel, U.; Becker, U.; Balazs, G.; Scheer, P.; Hönle, W.; Becker, M.; Jansen, M. *Eur. J. Inorg. Chem.* **2005**, 135–141.
- (15) Colson, A. C.; Whitmire, K. H. *Chem. Mater.* **2011**, *23*, 3731–3739.
- (16) (a) Kelly, A. T.; Rusakova, I.; Ould-Ely, T.; Hofman, C.; Lüttge, A.; Whitmire, K. H. *Nano Lett.* **2007**, *7*, 2920–2925. (b) Colson, A. C.; Chen, C.-W.; Morosan, E.; Whitmire, K. H. *Adv. Funct. Mater.* **2012**, *22*, 1850–1855.
- (17) (a) Panneerselvam, A.; Periyasamy, G.; Ramasamy, M.; Afzaal, K.; Malik, M. A.; O'Brien, P.; Burton, N. A.; Waters, J.; van Dongen, B. E. *Dalton Trans.* **2010**, *39*, 6080–6091. (b) Green, M.; Brien, P. O. *Adv. Mater.* **1998**, *10*, 527–528. (c) Buhro, W. E. *Polyhedron* **1994**, *13*, 1131–1148.
- (18) Dobbie, R. C. *Inorg. Nucl. Chem. Lett.* **1973**, *9*, 191–193.
- (19) Schumann, H.; Roesch, L.; Schmidt-Fritsche, W. *Chem.-Ztg.* **1977**, *101*, 156–157.
- (20) Keiter, R. L.; Keiter, E. A.; Mittelberg, K. N.; Martin, J. S.; Meyers, V. M.; Wang, J. G. *Organometallics* **1989**, *8*, 1399–1403.
- (21) Basato, M. *J. Chem. Soc., Dalton Trans.* **1985**, 91–97.
- (22) Dreher, C.; Zabel, Z.; Bodensteiner, M.; Scheer, M. *Organometallics* **2010**, *29*, 5187–5191.
- (23) Fischer, E. O.; Louis, E.; Kreiter, C. G. *Angew. Chem., Int. Ed.* **1969**, *8*, 377–378.
- (24) Guggenberger, L. J.; Klabunde, U.; Schunn, R. A. *Inorg. Chem.* **1973**, *12*, 1143–1148.
- (25) Huttner, G.; Schelle, S. *J. Organomet. Chem.* **1973**, *47*, 383–390.
- (26) Huttner, G.; Schelle, S. *J. Organomet. Chem.* **1969**, *19*, P9–P10.

- (27) Vogel, U.; Scheer, M. *Z. Anorg. Allg. Chem.* **2001**, *627*, 1593–1598.
- (28) Venkatraman, M.; Neumann, J. P. *Bull. Alloy Phase Diagrams* **1990**, *5*, 430–434.
- (29) (a) Blackman, C. S.; Carmalt, C. J.; Manning, T. D.; Parkin, I. P.; Apostolico, L.; Molloy, K. C. *Appl. Surf. Sci.* **2004**, *233*, 24–28.
(b) Zhou, Y.-N.; Xue, M.-Z.; Fu, Z.-W. *J. Power Sources* **2013**, *234*, 310–332.
- (30) Carpenter, J. P.; Lukehart, C. M.; Milne, S. B.; Stock, S. R.; Wittig, J. E.; Jones, B. D.; Glosser, R.; Zhu, J. G. *J. Organomet. Chem.* **1998**, *557*, 121–130.
- (31) Hens, Z.; Martins, J. C. *Chem. Mater.* **2013**, *25*, 1211–1221.
- (32) Lacroix, L.-M.; Lachaize, S.; Falqui, A.; Respaud, M.; Chaudret, B. *J. Am. Chem. Soc.* **2009**, *131*, 549–557.
- (33) WinDaisy, Version 4.05; Bruker-Franzen Analytik GmbH: Karlsruhe, Germany.
- (34) Davis, H. B.; Einstein, F. W. B.; Glavina, P. G.; Jones, T.; Pomeroy, R. K.; Rushmann, P. *Organometallics* **1989**, *8*, 1030–1039.
- (35) Uhlig, F.; Gremler, S.; Dargatz, M.; Scheer, M.; Hermann, E. *Z. Anorg. Allg. Chem.* **1991**, *606*, 105–108.
- (36) Werner, H.; Deckelmann, K.; Schoenenberger, U. *Helv. Chim. Acta* **1970**, *53*, 2002–2009.